

This is an author produced version of a paper published in *Acta Agriculturae Scandinavica*, Section B - Plant Soil Science. This paper has been peer-reviewed and is proof-corrected, but does not include the journal pagination.

Citation for the published paper:

Kätterer, T., Andrén, O. (2009) Predicting daily soil temperature profiles in arable soils in cold temperate regions from air temperature and leaf area index. *Acta Agriculturae Scandinavica, Section B - Plant Soil Science*. Volume: 59 Number: 1, pp 77-86.

<http://dx.doi.org/10.1080/09064710801920321>

Access to the published version may require journal subscription.  
Published with permission from: Taylor & Francis



Epsilon Open Archive <http://epsilon.slu.se>

**Predicting daily soil temperature profiles in arable soils in cold temperate regions from air temperature and leaf area index**

T. KÄTTERER and O. ANDRÉN

*Department of Soil Sciences, SLU, Uppsala, Sweden*

Correspondence: T. Kätterer, Department of Soil Sciences, SLU, P.O. Box 7014, SE-750 07 Uppsala, Sweden. Tel.: +46 18 672425. Fax: +46 18 672795. E-mail: [thomas.katterer@mv.slu.se](mailto:thomas.katterer@mv.slu.se)

## Abstract

Modelling of ecosystem processes often requires soil temperature as a driving variable. Since soil temperature measurements are seldom available for regional applications, they have to be estimated from standard meteorological data. The objective of this paper is to present a general, simple empirical approach for estimating daily depth profiles of soil temperature from air temperature and a surface cover index (*LAI*; leaf area index) mainly focusing on agricultural soils in cold temperate regions. Air and soil temperature data measured daily or every fifth day at one to six different depths was acquired from all meteorological stations in Sweden where such records are available. The stations cover latitudes from 55.65 to 68.42 N and mean annual air temperatures from +8.6 to -0.6 °C. The time series spanned between two and ten years. The soils at the stations cover a wide range of soil textures, including two organic soils. We calibrated the model first for each station and then for all stations together and the general parameterization only slightly decreased the goodness of fit. This general model then was applied to two treatments in a field experiment: bare soil and a winter rape crop. The parameters governing the influence of *LAI* on heat fluxes were optimized using this experiment. Finally, the model was validated using soil temperature data from two barley treatments differing in *LAI* taken from another field experiment. In general, the model predicted daily soil temperature profiles well. For all soils and depths at the meteorological stations, 95% of the simulated daily soil temperatures differed by less than 2.8 °C from measurements. The corresponding differences were somewhat higher for the validation data set (3.9 °C), but bias was still low. The model explained 95% of the variation in the validation data. Since no site-specific adjustments were made in the validation simulations, we conclude that the application of the general model

presented here will result in good estimates of soil temperatures under cold temperate conditions. The very limited input requirements (only air temperature and *LAI*) that are easily obtainable from weather stations and from satellites make this model suitable for spatial applications at catchment or regional scales.

**Key words:** *Empirical model, LAI, regional model, simulation.*

## **Introduction**

Soil temperature affects most soil processes and also plant growth. Spatially explicit predictions of soil temperature dynamics are needed for ecological applications and agricultural management. Together with chemical and physical characteristics of the soil organic material, soil temperature is one of the major variables controlling soil biological activity (e.g. Lundegård, 1927; Kätterer et al., 1998; Frank et al., 2002). Unfortunately, comprehensive soil temperature records are seldom available (Schaetzl et al., 2005) and have to be estimated from other information, usually standard meteorological data.

Mechanistic approaches for estimating soil temperatures are computationally demanding and they are also parameter intensive (Qin et al., 2002). Detailed knowledge of water retention curves, hydraulic and thermal conductivity functions, heat capacity, surface resistance etc. is usually lacking, so simpler empirical approaches are necessary for spatial applications. These models can provide good approximations of point-scale soil temperature measurements when estimated from standard meteorological measurements and basic soil and crop characteristics, e.g. obtained from satellites (Kang et al., 2000).

A number of empirical or semi-empirical soil temperature models have been proposed (e.g. Gupta et al., 1982; McCann et al., 1991; Paul et al., 2004; Rankinen et al., 2004; Bond-Lamberty et al., 2005 and papers cited therein). Many of these models are not sensitive to surface cover (e.g. McCann et al., 1991) and only a few consider the effect of snow cover on heat transfer (e.g. Rankinen et al., 2004). A sinusoidal function of time oscillating around an average value with an increasing phase shift and attenuation with depth is often used to describe large-scale soil temperature dynamics (Campbell, 1985), and seems to work well also at the field scale in warm temperate climates, if surface temperature is known (Wu & Nofziger, 1999). However, even under these conditions a bias is introduced when using air temperature as a driver (Wu & Nofziger, 1999).

In colder climates, these simple sinusoidal functions may adequately predict soil temperatures at greater depths ( $>0.5$  m), if the influence of snow and frost is of minor importance, and adjustments are made for surface cover (Paul et al., 2002). However, this approach is often too crude in topsoils, where biological activity is high, especially at inter-annual time scales (Paul et al., 2004).

Snow dynamics and frost were included in the approach presented by Rankinen et al. (2004), but vegetation was not considered as a modifier of the upper boundary, even though its influence on sensible and latent heat fluxes can be significant (Morrow & Friedl, 1998; Bond-Lamberty et al., 2005). Rankinen et al. (2004) also used air temperature instead of surface temperature, which may be too simplistic for applications in arable land. Moreover, their approach (equation 12 in their paper) leads to unrealistic estimates at shallow depths when temperature gradients are high, due the quadratic dependence on soil depth in the denominator.

The objective of this paper is to present a simple and consistent approach for estimating daily soil temperature from air temperature and a surface cover index, focusing on agricultural soils in cold temperate regions. This model will be incorporated in a model system for calculating soil carbon balances for arable soils (Andr  n et al., 2004), but can also be used for other spatial applications, e.g., in the context of precision agriculture.

## Material and methods

### *Model description*

We modified a semi-empirical model developed for spatial modelling (Kang et al., 2000) making it suitable for estimating soil temperature from air temperature records under cold temperature conditions. Their model combines principles of heat transfer physics with an empirical model proposed by Zheng et al. (1993) and estimates mean soil temperature ( $T$ ) at any depth ( $z$ ; cm) using the following equation:

$$T_t(z) = T_{t-1}(z) + [T_{surf} - T_{t-1}(z)] \exp \left[ -z \left( \frac{\pi}{k_s p} \right)^{1/2} \right] \exp(-k_{LB} LAI_t) \quad (1)$$

where  $t$  is time (day),  $T_{surf}$  is the apparent temperature at the soil surface (air temperature was used by Kang et al., 2000),  $k_s$  is the thermal diffusivity ( $\text{cm}^2 \text{s}^{-1}$ ),  $p$  is the period of temperature variation (s, in this case one year), and  $k_{LB}$  is the radiation extinction coefficient according to Lambert-Beer's Law, which governs the radiation transfer between atmosphere and soil as a function of leaf area ( $LAI$ ) or an equivalent thickness of litter on the soil surface.

The assumptions made by Kang et al. (2000), that soil temperature would not fall below freezing and no snow cover would occur, is of course inappropriate for

Scandinavian conditions. Instead, we corrected air temperature by a factor ( $s_{snow}$ ) when air temperature was below 0 °C, accounting for the low thermal conductivity of snow. To include the effect of surface cover on  $T_{surf}$  during the growing season, we used the following relationship between air temperature ( $T_{air}$ ) and  $T_{surf}$ :

$$T_{surf} = \begin{cases} T_{air} [s_1 + (1 - s_1) \exp(-s_2 (LAI - LAI_{ref}))] & ; T_{air} \geq 0 \\ s_{snow} T_{air} & ; T_{air} < 0 \end{cases} \quad (2)$$

Note that the upper part of this equation ( $T_{air} \geq 0$ ) is normalized for standard conditions (i.e.,  $T_{surf} = T_{air}$  when  $LAI = LAI_{ref}$ ), which is assumed to correspond to the standard conditions at the meteorological stations. Thus, calculations for the standard meteorological stations are not affected for  $T_{air} \geq 0$ . For non-standard conditions ( $LAI \neq LAI_{ref}$ )  $T_{surf}$  differs from  $T_{air}$  to an extent governed by parameters  $s_1$  and  $s_2$ . Equations 1 and 2 represent the whole model, which is slightly modified below (Equation 7).

### *Study sites and data acquisition*

Air and soil temperature measured daily or at five-day intervals at one to six different depths were acquired from all meteorological stations in Sweden where soil temperature records are available. The stations cover latitudes from 55.65 to 68.42 N with mean annual air temperatures from +8.6 to -0.6 °C (Table I). The time series range from 2 to 10 years. The soils at the stations cover a wide range of soil textures, including two organic soils. No detailed information on vegetation cover at the various stations was available, so vegetation cover was set to a standard leaf area ( $LAI_{ref}$ ).

For evaluating the impact of vegetation on radiation transfer, we used two data sets from field experiments. The first experimental data set was derived from a French

site (data are freely available at <http://www-bioclim.grignon.inra.fr/ecobilan/base/welcome.html>; Gosse et al., 1999). We used the data from bare soil and the high N winter rapeseed treatment. *LAI* was calculated from *GAI* measurements as described below.

The second data set was taken from a comprehensive field study conducted in Sweden (Andrén et al., 1990). We used data from two barley plots, one treatment fertilized with nitrogen and one unfertilized. Temperature measurements were obtained for two growing seasons (from May 1981 to August 1982) from Alvenäs et al. (1986). Green area index (*GAI*; the area of all plant parts that are visibly green including stems and ears (only one side of leaves is counted) was used as a proxy for an apparent leaf area index (*LAI*) which also includes standing dead plant material and litter. *GAI* was measured during one growing season in the two barley treatments (Pettersson, 1989). Since the maximum *GAI* values during the growing season often correlate closely with grain yield (Olesen et al., 2002), we used measured grain yields to calculate maximum *GAI* for the two years considered here (Hansson et al., 1987; Pettersson, 1989). A non-linear function was fitted to the *GAI* data during the first half of the growing season, when  $LAI=0.8 \cdot GAI$  according to Flink et al. (1995) (Figure 1). *GAI* and *LAI* were set to zero before emergence of the barley crop in spring and after soil tillage in autumn. During grain filling (days 198-213), we let *LAI* decrease to 70% of its maximum value. This value was kept constant during maturation until crop harvest (day 244), when it dropped to 20% of maximum *LAI*, which is assumed to represent stubble and harvest residues. At the first post-harvest tillage, *LAI* dropped to zero (Figure 1).

*Calculation of mean daily soil temperature*



In our data set from the Swedish meteorological stations, only one meteorological station (Dingle) reports two daily soil temperature measurements, 7 a.m. and 7 p.m. at 5, 10 and 20 cm depth. At the other stations, temperature records are only available at 7 a.m. Averaged over a 7-year period, the morning records at Dingle were 0.89, 0.73 and 0.24 °C lower at 5, 10 and 20 cm depth, respectively, than the arithmetic mean of the morning and afternoon measurement. These differences showed seasonal patterns and were higher during summer (higher temperatures) than during winter. To correct for this seasonal bias, we regressed these differences on morning soil temperature records for all days where temperatures were above 0 °C (Figure 2). During these days, the bias was significantly related to temperature. Since both the slopes and intercepts of the regressions at each depth (for temperatures above 0 °C) were highly correlated with soil depth and the intercepts were almost identical to the constant bias estimated for temperatures below 0 °C, we fitted a response surface for estimated mean daily soil temperatures ( $T$ ) from soil depth and soil temperature measured at 7 a.m. ( $T_{7am}$ ). According to this model

$$T(z) = \begin{cases} 0.32 - 0.0128z + (1.1 - 0.004z)T_{7am} & ; \quad T_{7am} \geq 0 ; 0 < z \leq 25cm \\ T_{7am} - 0.0128z + 0.318 & ; \quad T_{7am} < 0 ; 0 < z \leq 25cm \\ T_{7am} & ; \quad z > 25cm \end{cases} \quad (3)$$

$T_{7am}$  can be assumed to represent mean daily soil temperature for depths below  $z=25$  cm.

### *Calibration and validation*

The heat transfer model (Equations 1 and 2) was calibrated and validated as follows: first we used equation 3 to calculate  $T$  from  $T_{7am}$  for the meteorological stations where only morning measurements were available (all except Dingle; Table II). Thereafter,

we applied the model to all 11 data sets using the parameter values proposed by Kang et al. (2000), i.e.,  $k_s=0.005$ ,  $p=365\times24\times60\times60$ , and  $k_{LB}=0.45$ , and assuming that  $LAI=3$  represented the vegetation at the meteorological stations. The results showed that the propagation of daily changes and phase shift with depth were not in accordance with the measurements, as demonstrated for the coldest site (Katterjåkk) at 1m depth (Figure 3). Therefore, we considered both parameters in equation 1 ( $k_s$  and  $k_{LB}$ ) as free parameters and estimated their values for each site separately by minimizing the differences between predicted and measured values for days when soil temperatures were above zero. In the same way, we estimated  $s_{snow}$  (Equation 2) for temperatures below zero for the three sites where soil temperatures were measured at 5 cm depth (Dingle, Lanna and Uppsala). Thereafter, we estimated common values for the parameters  $k_s$  and  $k_{LB}$  for all sites and soil depths and investigated their impact on error statistics.

Secondly, the values of parameters  $s_1$  and  $s_2$  (Equation 2) were set to 0.95 and 0.40, respectively. For example at a mean daily air temperature of 10 °C, this means that  $T_{surf}$  is 1.6 °C higher than  $T_{air}$  on bare soil and 0.4 °C lower under very dense ( $LAI=8$ ) vegetation (Figure 4). The rationale for this difference is that surface temperatures on bare soil often are higher than air temperatures due to intercepted radiation. On the other hand, the shading of vegetation will result in lower surface temperatures compared to air. This is supported by many studies. For example, a study in the warm temperate zone showed that  $T_{surf}$  on a bare soil on average over three years was about 2°C higher than  $T_{air}$  (Wu & Nofziger, 1999). In a Swedish study, soil temperatures at 5 cm depth were in average during June and July 1.1 or 1.7 °C higher under unfertilized than under fertilized barley during two consecutive years (Alvenäs, 1986). Rochette et al. (1992) observed higher CO<sub>2</sub> production in summer

fallow plots, where the contribution of root respiration was negligible, than in plots cropped to barley. This was attributed to lower soil temperature (shading) and water content (transpiration) under barley than under fallow. In the French data set we used in our study, surface temperature on average was 0.4 °C higher on bare soil and 0.6 °C lower under dense rapeseed compared with air temperature (Gosse et al., 1999).

Thirdly, the model as parameterized for the meteorological stations was applied to the bare soil and high N rapeseed treatments from the French experiment (Gosse et al., 1999).  $LAI$  was adjusted according to the measured  $GAI$  as described above. The simulations revealed that the calculated differences in  $T$  between these two treatments were strongly overestimated. Therefore, we propose an attenuation of the temperature gradient between air and soil, irrespective of  $LAI$ . We therefore partitioned the attenuation factor in equation 1 ( $\exp(-k_{LB} LAI)$ ) into two, one part that is dependent on  $LAI$  ( $\exp(-k_{lai} LAI)$ ) and one that is not ( $\alpha$ ). The attenuation factor in equation 1 thus becomes  $\alpha \cdot \exp(-k_{lai} LAI)$ , which equals  $\exp(-k_{LB} LAI)$  under standard conditions. We estimated the values of these parameters by fitting the model to observed soil temperatures at 5 cm depth under bare soil and the high N rapeseed treatment. This partitioning is also supported by the very high estimated values of  $k_{LB}$  in the calibration for the meteorological stations (Table III).

Finally, the two barley treatments from the Swedish experiment were used for validation.  $LAI$  in the two treatments was set according to measurements as described above (Figure 1). Thereafter, the model calibrated for the French data set as described above was used to simulate soil temperatures in these two treatments.

### *Statistical measures*

In the calibration and validation, we used mean absolute error (*MAE*) as a criterion for goodness of fit.

$$MAE = \frac{\sum_{i=1}^n |P_i - O_i|}{n} \quad (4)$$

where  $P_i$  and  $O_i$  are predicted and observed values, respectively, and  $n$  is the number of observations.

Besides the coefficient of determination ( $R^2$ ) obtained from linear regression, we also present the root mean square error (*RMSE*):

$$RMSE = \sqrt{\frac{\sum_{i=1}^n (P_i - O_i)^2}{n}} \quad (5)$$

The RMSE reflects the magnitude of the mean difference between observations and predictions but does not indicate if the estimate is biased. To quantify a systematic bias, we calculated also the mean bias error (*MBE*):

$$MBE = \frac{\sum_{i=1}^n (P_i - O_i)}{n} \quad (6)$$

A positive value of *MBE* indicates over-prediction and a negative value indicates under-prediction.

## Results and discussion

### *Surface temperature*

The calculated mean annual surface temperatures were between 0.1 (southern Sweden) to 3.2°C (northern Sweden) higher than mean annual air temperatures (Table II). Naturally, these differences increase with latitude due to the longer winters with

snow cover. However, also during summer, temperatures often were higher at 5cm depth than in the air, and mean annual soil temperatures at all depths were more similar to the estimated values of  $T_{surf}$  than to mean annual air temperatures (Table II).

The need for correction of the original model proposed by Kang et al. (2000) during winter was obvious (Figure 3). Our simple approach to estimate surface soil temperatures during winter yielded reasonable results (Table III). The estimated parameter value ( $s_{snow}=0.20$ ; Table IV) means that soil surface temperature is 20% of air temperature (in °C) at sub-zero air temperatures.

### *Soil temperature*

Daily mean values calculated from two soil temperature measurements, either from daily maximum and minimum temperature or from one morning and one afternoon observation can be considered as unbiased estimates of daily mean soil temperature (Hu & Feng, 2003). In their study, daily mean soil temperature calculated from one morning and one afternoon observation remained within 0.15 °C of the daily mean calculated from 24-hourly data at different stations in the USA. However, the same work also showed that single daily measurements at shallow depth do not satisfactorily represent mean daily soil temperature, just as in our case.

Estimated mean annual soil temperatures deviated by less than 1.5°C from the measurements when the model was fitted to each site separately (Table II). In average over all sites and depths, measured and estimated soil temperatures differed by less than 0.01 °C. The highest deviation (1.5 °C at Alnarp) was due to missing data during the winter of 1991/1992. The two fitted parameters  $k_{BL}$  and  $k_s$  for the nine sites with mineral soils were strongly correlated (Pearson's  $r = 0.89$ ). Re-running the model with

average parameter values for these sites resulted in slightly poorer model fits (Table III). Differences between site-specific calibrated simulations and the general model were small at shallow depths. For topsoils (0-20 cm)  $R^2$  decreased by less than 1.6% and on average over all sites by less than 1%. The impact on changes in phase shift with depth, governed by the parameter  $k_s$ , however became more significant at greater depths (Figure 5; sub-figure for 235 cm depth). On average over all sites, *MAE*, *MBE* and *RMSE* increased by between 0.0 and 0.6 °C at depths down to 1 m (0.1°C on average) and by 0.4 to 0.9°C at 2.35 m depth (only one site).  $R^2$  values decreased by between 0.00 and 0.06. The dynamics of measured and simulated soil temperatures for one site are shown in Figure 5. For all soils and depths at the meteorological stations, 95% of the simulated daily soil temperatures differed by less than 2.8 °C from measurements. Compared to previous work, this model error is quite small (e.g. Gupta et al., 1982). From these results we conclude that the application of this general model will result in reasonable estimates of soil temperature under Swedish conditions with *MAE*, *MBE* and *RMSE* of less than 2°C (average 1.2°C), 1.5°C (average 0.3°C) and 2.2°C (average 1.4°C), respectively. For the organic soils, we propose different parameter values accounting for the higher heat capacity in these soils (Table IV).

The partitioning of the attenuation factor into a *LAI*-dependent and an independent term resulted in the following parameter values:  $\alpha=0.24$  and  $k_{lai}=0.15$  (Table IV). The model fit to the French data set was reasonably good (*MAE* was 1.3°C and *MBE* was -0.7 °C under both bare soil and winter rapeseed and *RMSE* was 1.6 and 1.7 °C, respectively) and the simulated differences in soil temperature between the two treatments were the same as the measured (0.9°C) on average over the measurement period (Figure 6). Deviations between measurements and simulations at

the end of the growing period were probably due to dry soil conditions (Gosse et al., 1999), which probably resulted in higher surface temperatures in the fallow treatment and higher energy input to the fallow soil due to lower evaporative cooling in fallow than under the rapeseed crop. The general model explained 90 and 85% of the variation in soil temperatures under bare soil and winter rapeseed, respectively.

The resulting modified model that we propose here to be valid also for agricultural soils in cold temperate regions thus becomes:

$$T_t(z) = T_{t-1}(z) + [T_{surf} - T_{t-1}(z)] \alpha \exp(-k_z z) \exp(-k_{lai} LAI_t) \quad (7)$$

where

$$k_z = \left( \frac{\pi}{k_s p} \right)^{1/2} \quad (8)$$

and where  $T_{surf}$  is defined in equation 2. The estimated parameter values for this general model are presented in Table IV and the soil depth and surface cover dependent damping factor ( $= \alpha \exp(-k_z z) \exp(-k_{lai} LAI)$ ) is visualized in Figure 7.

The application of this model to the validation data resulted in a relatively good model fit for barley. The model explained 95% of the variation in both treatments. Over the measured period, *MAE*, *MBE* and *RMSE* were 1.4, 0.0 and 1.8°C and 1.2, -0.2 and 1.7°C in unfertilized and fertilized barley, respectively. During the two summers (June and July) however, the simulated mean difference between the two treatments was lower than the measured, by 0.7 and 1.4°C, respectively (Figure 8).

We did not have access to any independent test data for organic soils. However, we think that the differences in soil temperatures between mineral and organic soils as estimated for the meteorological stations are reasonable and agree

with common knowledge. Assuming that the influence of surface cover as quantified for mineral soils also applies to these soils (parameters  $s_1$ ,  $s_2$  and  $k_{lai}$ ), differences between the two soil types are expressed in the parameter  $\alpha$  and  $k_z$  (Table IV). The measured and simulated differences between the organic and sandy soil at Flahult are shown in Figure 9.

The model should be further tested at sites for which comprehensive *LAI* measurements are available and under different climatic conditions. For field applications, site-specific calibration would of course improve the accuracy of predictions. However, the minimal data requirement of the general model makes it useful for regional applications where biophysical information is scarce.

In general, the model predicted the measured daily soil temperature profiles well. Differences between predicted and measured soil temperature were largest during periods with strong fluctuations of air temperature. For all soils and depths at the meteorological stations, 95% of the simulated daily soil temperatures differed by less than 2.8 °C from measurements. The corresponding differences were somewhat larger at the French site (3.1 °C) and for the validation data set (3.9 °C) but the bias was still small. Since no site-specific adjustments of model parameters were made in the validation simulations, we conclude that the application of the general model presented here will result in satisfactory estimates of soil temperatures under cold temperate conditions.

## **Acknowledgements**

The Swedish Meteorological and Hydrological Institute is acknowledged for providing air and soil temperature data. Financial support was provided from the



Swedish Farmers' Foundation for Agricultural Research and the Swedish Research Council for Environment, Agricultural Sciences and Spatial Planning (FORMAS).

## References

- Alvenäs, G., Johnsson, H., & Jansson, P.-E. (1986). Meteorological conditions and soil climate of four cropping systems. Measurements and simulations from the project “Ecology of Arable Land”. Swedish University of Agricultural Sciences, Department of Ecology and Environmental Research. *Report 24*.
- Andrén, O., Kätterer, T., & Karlsson, T. (2004). ICBM regional model for estimations of dynamics of agricultural soil carbon pools. *Nutrient Cycling in Agroecosystems*, 70, 231-239.
- Andrén, O., Lindberg, T., Paustian, K., & Rosswall, T. (Eds). (1990). Ecology of Arable Land – Organisms, Carbon and Nitrogen Cycling. *Ecological Bulletins* 40 (Copenhagen).
- Bond-Lamberty, B., Wang, C., & Gower, S.T. (2005). Spatiotemporal measurement and modelling of stand-level boreal forest soil temperatures. *Agricultural and Forest Meteorology*, 131, 27-40.
- Campbell, G.S. (1985). *Soil Physics with Basic: Transport Models for Soil-Plant Systems*. Elsevier, Amsterdam.
- Flink, M., Pettersson, R., & Andrén, O. (1995). Growth dynamics of winter wheat in the field with daily fertilization and irrigation. *Journal of Agronomy and Crop Science*, 174, 239-252.
- Frank, A.B., Liebig, M.A., & Hanson, J.D. (2002) Soil carbon dioxide fluxes in northern semiarid grasslands. *Soil Biology & Biochemistry*, 34, 1235-1241.
- Gosse, G., Cellier, P., Denoroy, P., Gabrielle, B., Laville, P., Leviel, B., Justes, E., Nicolardot, B., Mary, B., Recous, S., Germon, J.-C., Hénault, C., & Leech,

- P.K. (1999). Water, carbon and nitrogen cycling in a rendzina soil cropped with winter oilseed rape: the Châlons Oilseed Rape Database. *Agronomie*, 19, 119-124.
- Gupta, S.C., Radke, J.K., Larson, W.E., & Shaffer, M.J. (1982). Predicting temperatures of bare- and residue-covered soils from daily maximum and minimum air temperatures. *Soil Science Society of America Journal*, 43, 372-376.
- Hansson, A.-C., Pettersson, R., & Paustian, K. (1987). Shoot and root production and nitrogen uptake in barley, with and without nitrogen fertilization. *Journal of Agronomy and Crop Science*, 158, 163-171.
- Hu, Q., & Feng, S. (2003). A daily soil temperature dataset and soil temperature climatology of the contiguous United States. *Journal of Applied Meteorology*, 42, 1139-1156.
- Kang, S., Kim, S., Oh, S., & Lee, D. (2000). Predicting spatial and temporal patterns of soil temperature based on topographic, surface cover and air temperature. *Forest Ecology and Management*, 136, 173-184.
- Kätterer, T., Reichstein, M., Andrén, O., & Lomander, A. (1998). Temperature dependence of organic matter decomposition: A critical review using literature data analysed with different models. *Biology and Fertility of Soils*, 27, 258-262.
- Lundegård, H. (1927). Carbon dioxide evolution of soil and crop growth. *Soil Science*, 23, 417-453.

- McCann, I.R., McFarland, M.J., & Witz, J.A. (1991). Near-surface bare soil temperature model for biophysical models. *Transactions of the American Society of Agricultural Engineers*, 34, 748-755.
- Morrow, N., & Friedl, M.A. (1998). Modeling biophysical controls on land surface temperature and reflectance in grasslands. *Agricultural and Forest Meteorology*, 92, 147-161.
- Olesen, J.E., Petersen, B.M., Berntsen, J., Hansen, S., Jamieson, P.D., & Thomsen, A.G. (2002). Comparison of methods for simulating effects of nitrogen on green area index and dry matter growth in winter wheat. *Field Crops Research*, 74, 131-149.
- Paul, K.I., Polglase, P.J., O'Connell, A.M.O., Carlyle, C.J., Semthurst, P.J., & Khanna, P.K. (2002). Soil nitrogen availability predictor (SNAP): a simple model for predicting mineralization of nitrogen in forest soils. *Australian Journal of Soil Research*, 40, 1011-1026.
- Paul, K.I., Polglase, P.J., Semthurst, P.J., O'Connell, A.M.O., Carlyle, C.J., & Khanna, P.K. (2004). Soil temperature under forests: a simple model for predicting soil temperature under a range of forest types. *Agricultural and Forest Meteorology*, 121, 167-182.
- Pettersson, R. (1989). Above-ground dynamics and net production of spring barley in relation to nitrogen fertilization. *Swedish Journal of Agricultural Research*, 19, 135-145.
- Qin, Z., Berliner, P., & Karnieli, A. (2002). Numerical solution of a complete surface energy balance model for simulation of heat fluxes and surface temperature

- under bare soil environment. *Applied Mathematics and Computation*, 130, 171-200.
- Rankinen, K., Karvonen, T., & Butterfield, D. (2004). A simple model for predicting soil temperature in snow-covered and seasonally frozen soil: model description and testing. *Hydrology and Earth System Sciences*, 8, 706-716.
- Rochette, P., Desjardins, R.L., Gregorich, E.G., Pattey, E., & Lessard, R. (1992). Soil respiration in barley (*Hordeum vulgare* L.) and fallow fields. *Canadian Journal of Soil Science*, 72, 591-603.
- Schaetzl, R.J., Knapp, B.D., & Isard, S.A. (2005). Modeling soil temperatures and the mesic-frigid boundary in the Central Great Lakes region, 1951-2000. *Soil Science Society of America Journal*, 69, 2033-2040.
- Wu, J., & Nofziger, D.L. (1999). Incorporating temperature effects on pesticide degradation into a management model. *Journal of Environmental Quality*, 28, 92-100.
- Zheng, D., Hunt Jr. E.R., & Running, S.W. (1993). A daily soil temperature model based on air temperature and precipitation for continental applications. *Climate Research*, 2, 183-191.

## Tables

Table I. Soil types, mean annual temperatures ( $T_{air}$ ) during the time periods (2 to 10 years) at which soil temperatures were recorded every 5<sup>th</sup> day (period in *italics*) or every day at the meteorological stations (from south to north).

Station	Soil type	$T_{air}$	Period	Latitude (N)	Longitude (E)
Alnarp	Loam	8.6	1991-1992	55° 39'	13° 05'
Flahult1	Peat	6.1	<i>1996-2003</i>	57° 41'	14° 09'
Flahult2	Sand	6.1	<i>1996-2003</i>	57° 41'	14° 09'
Lanna*	Clay	7.3	1996-2004	58° 21'	13° 08'
Dingle	Sandy clay	7.0	<i>1996-2002</i>	58° 32'	11° 34'
Ultuna	Clay loam	6.6	1996-2005	59° 49'	17° 39'
Avesta	Clay	6.1	<i>1996-2002</i>	60° 08'	16° 10'
Lännäs	Silt Loam	3.9	1996-2004	63° 10'	17° 40'
Abisko1	Peat	0.3	<i>1996-2005</i>	68° 21'	18° 49'
Abisko2	Glacial till	0.3	<i>1996-2005</i>	68° 21'	18° 49'
Katterjåkk	Loamy sand	-0.6	1996-2004	68° 25'	18° 10'

\*For Lanna, air temperatures were taken from a nearby station (Längjum 58° 13' N, 13° 04' E)

Table II. Mean annual air temperatures ( $T_{air}$ ; cf. Table I), surface temperatures ( $T_{surf}$ ), soil types and measured and calculated mean annual soil temperatures ( $^{\circ}\text{C}$ ) at the meteorological stations.

Sation	Soil type		$T_{air}$	$T_{surf}$	Soil temperature at different depths (cm)					
					5	10	20	50	100	235
Alnarp*	Loam	measured	8.6			9.8	10.3	9.6	9.5	
		calculated		8.7		8.8	8.8	8.8	8.8	
Flahult1	Peat	measured	6.1				6.9	6.7	6.7	
		calculated		6.9			6.9	6.9	6.9	
Flahult2	Sand	measured	6.1				7.5	7	6.9	
		calculated		6.9			6.9	6.9	6.9	
Lanna	Clay	measured	7.3		8.1	8	7.9	7.6		
		calculated		7.8	7.8	7.8	7.8	7.8		
Dingle	Sandy clay	measured	7.0		8	8.2	8.2	8.3	8.2	
		calculated		7.6	7.6	7.6	7.6	7.6	7.6	
Ultuna	Clay loam	measured	6.6		7.7	7.7	7.8	7.4	7.4	6.9
		calculated		7.4	7.4	7.4	7.4	7.4	7.4	7.3
Avesta	Clay	measured	6.1					6.8		
		calculated		7.0				7.1		
Lännäs		measured	3.9			5.4			5.8	
		calculated		5.7		5.7			5.7	
Abisko1	Peat	measured	0.3				3.2	2.8	3	
		calculated		3.2			3.3	3.2	3.2	
Abisko2	Till	measured	0.3				2.3	2.2	2	
		calculated		3.2			3.2	3.2	3.2	
Katterjåkk	Loamy sand	measured	-0.6					2.4	2.7	
		calculated		2.6				2.6	2.6	

\*missing data during winter resulted in biased measured means.

Table III. Fitted parameter values ( $k_{LB}$  and  $k_s$ ) and the calibration errors for the sites expressed as mean absolute error (MAE). root mean squared error (RMSE). mean bias error (MBE) and coefficient of determination ( $R^2$ ; linear regression) according to equations 1 and 2 using average parameter values for organic and mineral soils.

Station	$k_{LB}$	$k_s$ (*10 <sup>-4</sup> )	MAE						RMSE						MBE						$R^2$					
			Depth (cm)						Depth (cm)						Depth (cm)						Depth (cm)					
			5	10	20	50	100	235	5	10	20	50	100	235	5	10	20	50	100	235	5	10	20	50	100	235
Alnarp*	0.57	3.6		1.2	1.5	0.9	1.2			1.5	1.7	1.1	1.4			1.2	1.5	0.9	1.2			0.97	0.98	0.98	0.95	
Flahult1	0.97	4.7			1.0	1.2	1.1				1.3	1.4	1.3				0.0	-0.2	-0.1				0.96	0.95	0.88	
Flahult2	0.8	5.4			1.0	1.1	1.2				1.3	1.3	1.4				0.6	0.2	0.0				0.97	0.98	0.97	
Lanna	0.47	1.5	1.1	1.0	0.9	1.0			1.4	1.8	1.2	1.8			1.1	1.0	0.9	1.0			0.96	0.93	0.90	0.91		
Dingle	0.42	2	1.8	1.8	1.5	1.1	0.8		2.2	2.2	1.9	1.4	1.0		0.4	0.6	0.6	0.7	0.4		0.96	0.96	0.97	0.97	0.97	
Ultuna	0.9	7.4	1.1	1.0	0.9	1.0	0.8	0.5	1.3	1.2	1.2	1.2	1.0	0.6	1.1	1.0	0.9	1.0	0.8	0.5	0.95	0.95	0.95	0.94	0.97	0.97
Avesta	0.53	0.9				1.4						1.2						-0.3						0.95		
Lännäs	0.71	3.7		1.1			1.1			1.5			1.3			-0.7			0.1			0.96				0.97
Abisko1	0.99	3.2			1.8	2.0	1.6				1.7	1.9	1.3				0.0	-0.4	-0.2				0.87	0.79	0.79	
Abisko2	0.66	2.4			1.2	1.3	1.5				1.6	1.6	1.8				-1.0	-1.0	-1.2				0.94	0.95	0.92	
Katterjåkk	0.53	3.4				0.9	1.0					1.1	1.3					-0.2	0.0					0.95	0.91	
Average1 **	0.62	3.37	1.3	1.2	1.2	1.1	1.1	0.5	1.6	1.5	1.5	1.3	1.3	0.6	0.8	0.6	0.6	0.3	0.2	0.5	0.96	0.95	0.95	0.95	0.95	0.97
Average2**	0.98	3.95			1.4	1.6	1.4				1.5	1.7	1.3				0.0	-0.3	-0.2				0.91	0.87	0.83	

\*missing data during winter resulted in biased measured means.

\*\*Average1 corresponds to organic soils (Flahult1 and Abisko1) and Average2 corresponds to mineral soils.



Table IV.

Estimated parameter values for the general model for mineral and organic soils

Parameter	Mineral soils	Organic soils
$\alpha$	0.24	0.11
$k_z$	0.017	0.016
$k_{lai}$	0.15	0.15
$s_1$	0.95	0.95
$s_2$	0.40	0.40
$s_{snow}$	0.20	0.20
$LAI_{ref}$	3.0	3.0

## Figure captions

Figure 1. Measured (symbols) green area index ( $GAI$ ) in fertilized spring barley during one growing season (data from Pettersson. 1989) and the proposed representation of leaf area index ( $LAI$ ; solid line) as described in the text. which increases with  $GAI$  (dashed line) and declines after its maximum to 70% of its maximum value before harvest.  $LAI$  is assumed to be 20% of its maximum value between harvest and soil tillage.

Figure 2. Differences between soil temperatures measured at 7 a.m. ( $T_{7am}$ ) and daily mean soil temperature ( $T$ ) at 5, 10 and 20 cm depth at Dingle regressed on  $T_{7am}$ . The line represents the model used for de-trending (Equation 3). All slopes for  $T_{7am} > 0$  °C are highly significant.

Figure 3. Measured (bold grey line) and simulated (black line) soil temperatures at 100 cm depth at Katterjåkk in Northern Sweden using the parameter values proposed by Kang et al. (2000).

Figure 4. Surface temperature ratio ( $T_{surf}/T_{air}$ ; cf. Equation 2) for air temperatures above 0 °C as a function of leaf area index ( $LAI$ ) including surface litter.

Figure 5. Air temperature and soil temperatures at different depths at Ultuna in Central Sweden; bold grey lines represent measurements and black lines represent

simulations using the general model (average parameter values). The results from the site-specific calibrated simulations are also shown for 235 cm depth.

Figure 6. Measured (symbols) and simulated (line) differences in daily mean soil temperature at 5 cm depth between bare soil and a high N winter rape treatment. Data from Gosse et al. (1999).

Figure 7. The damping factor ( $= \alpha \exp(-k_z z) \exp(-k_{lai} LAI)$ ) as a function of leaf area index ( $LAI$ ) and soil depth.

Figure 8. Differences in measured (symbols) and simulated (line) daily mean soil temperatures at 5 cm depth between unfertilized and fertilized barley in a Swedish field experiment (data from Alvenäs. 1986).

Figure 9. Impact of soil type on soil temperature at 20 cm depth during one year at Flahult: measured (symbols) and simulated (line) differences in mean daily soil temperatures between peat and sandy soil. Note that peat soil is colder than sandy soil during the growing season and warmer during winter.

## Figures

Figure 1

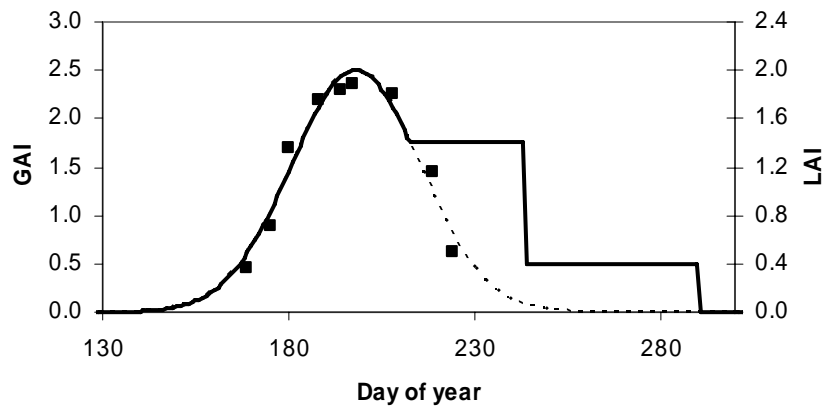


Figure 2

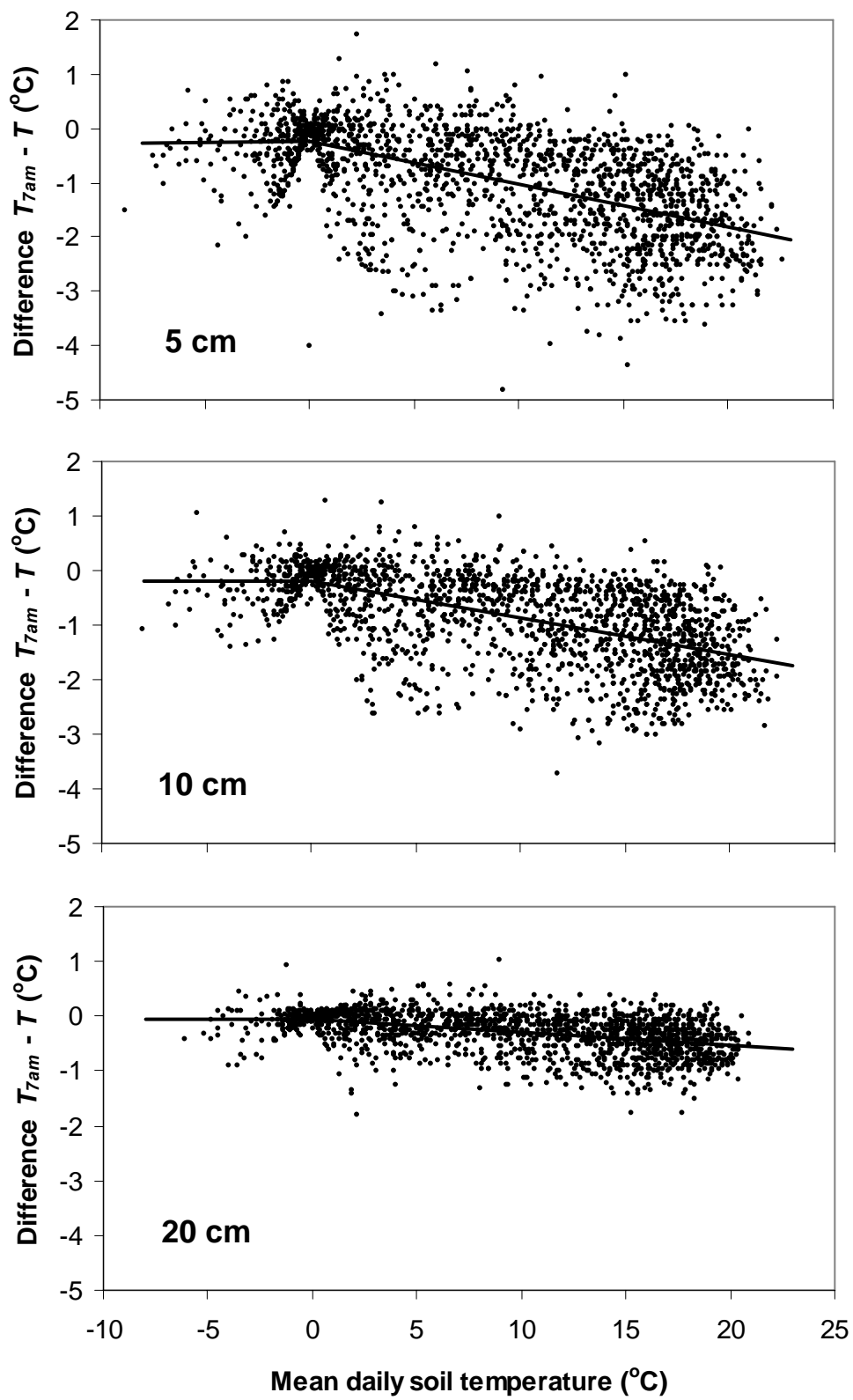


Figure 3

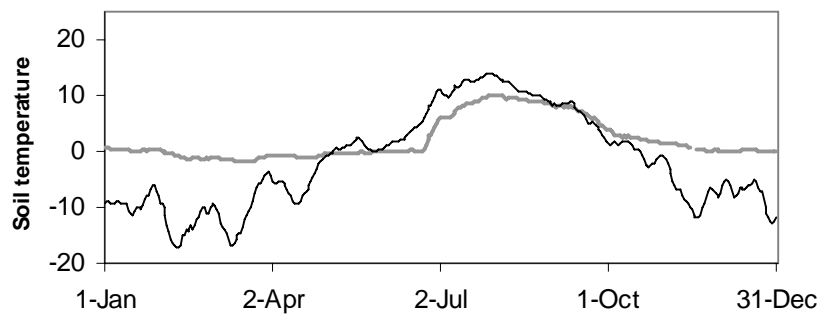


Figure 4

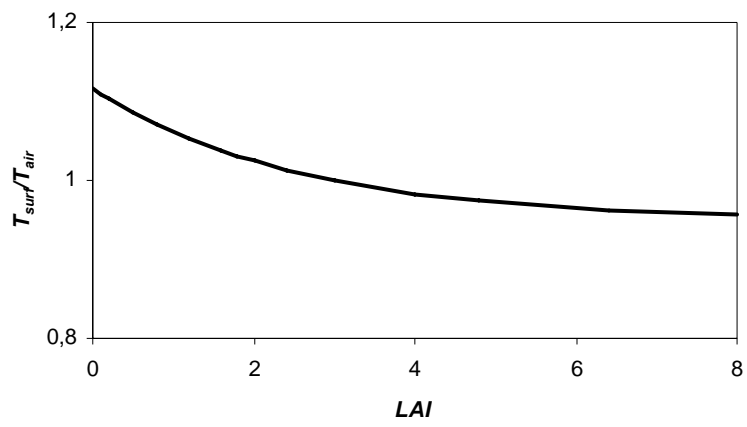


Figure 5

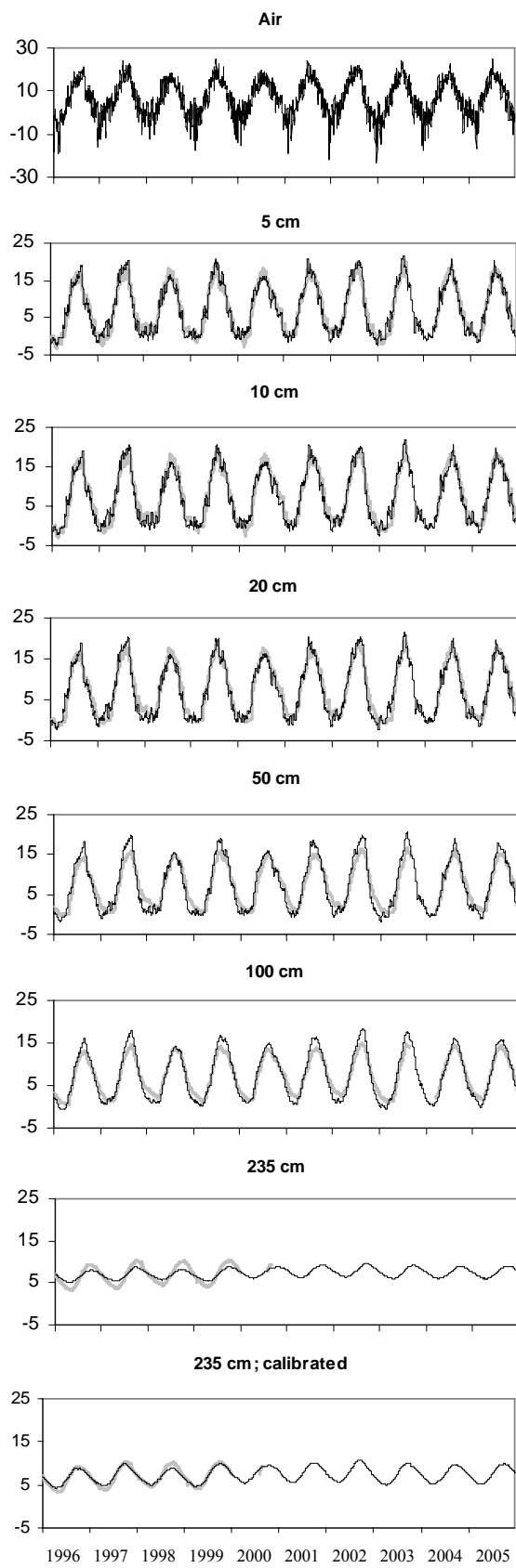




Figure 6

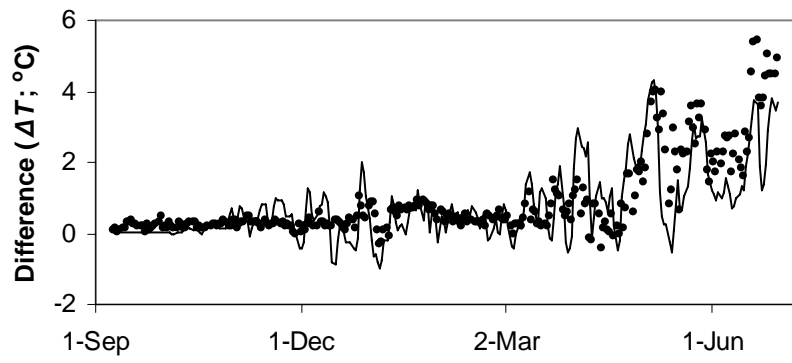


Figure 7

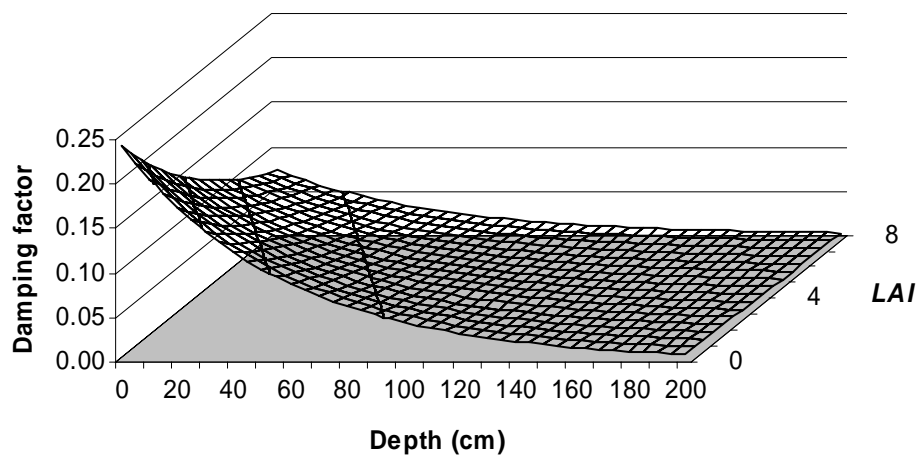


Figure 8

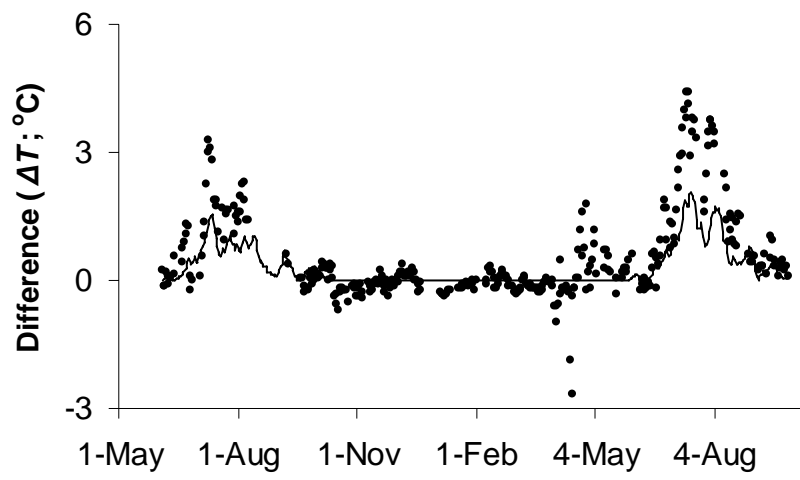


Figure 9

